18

Using Artificial Neural Networks to Identify Glaucoma Stages

Gustavo Santos-García and Emiliano Hernández Galilea
Department of Surgery. Faculty of Medicine, Universidad de Salamanca
Spain

1. Introduction

Glaucoma is one of the principal causes of blindness in the world[1]. It is an illness which has an asymptomatic form until advanced stages, thus early diagnosis represents an important objective to achieve with the aim that people who present Glaucoma maintain the best visual acuity throughout life, thereby improving their quality of life.
An Artificial Neural Network (ANN) is proposed for the diagnosis of Glaucoma. Automated combination and analysis of information from structural and functional diagnostic techniques were performed to improve Glaucoma detection in the clinic.
In our work we contribute the inclusion of Artificial Intelligence and neuronal networks in the diverse systems of clinical exploration and autoperimetry and laser polarimetry, with the objective of facilitating the adequate staging in a rapid and automatic way and thus to be able to act in the most adequate manner possible.
Data from clinical examination, standard perimetry and analysis of the nerve fibers of the retina with scanning laser polarimetry (NFAII;GDx) were integrated in a system of Artificial Intelligence. Different tools in the diagnosis of Glaucoma by an automatic classification system were explained based on ANN. In the present work an analysis of 106 eyes, in accordance with the stage of glaucomatous illness was used to develop an ANN. Multilayer perceptron was provided with the Levenberg-Marquardt method. The learning was carried out with half of the data and with the training function of gradient descent w/momentum backpropagation and was checked by the diagnosis of a Glaucoma expert ophthalmologist. A correct classification of each eye in the corresponding stage of Glaucoma has been achieved. Specificity and sensitivity are 100%. This method provides an efficient and accurate tool for the diagnosis of Glaucoma in the stages of glaucomatous illness by means of AI techniques.

2. Clinical, structural and functional examination in Glaucoma

Glaucoma is one of the principal causes of blindness in the world. Glaucoma is an ocular disease and it is the second leading cause of blindness worldwide and responsible for 20% of blindness in Europe. Glaucoma is also an age related disease and has age-adjusted prevalence of 1.55%, therefore the increase in elderly population in the world will increase the number of patients with Glaucoma in the coming decades. This increase in patients with Glaucoma will enlarge the socioeconomic cost associated to visual deficient diseases. Therefore efforts should

[1] Research supported by Spanish project DESAFIOS10 TIN2009-14599-C03-01.

be made to improve the diagnosis and treatment of this disease (European Glaucoma Society, 2008; Gordon et al., 2002; Huang & Chen, 2005; Quigley, 1985).

Glaucoma is an optic neuropathy characterized by progressive loss of retinal ganglion cells, changes in the optic nerve head and associated visual field loss (Fig. 1). There are a variety of risk factors for Glaucoma, the most important of which is intraocular pressure, IOP (Quigley et al., 1994). Primary open angle Glaucoma has an adult onset, is usually bilateral, and has no symptoms until late in the disease when patients lose their central vision. An understanding of the etiology and anatomical changes associated with Glaucoma is critical for early diagnosis of the disease and preserving sight (Song et al., 2005). Different studies have shown that structural and functional techniques for detecting Glaucoma often identify different Glaucoma patients when Glaucoma severity is not too advanced (Bowd et al., 2001; Zangwill et al., 2001), and that combining structural and functional techniques can improve Glaucoma detection (Caprioli, 1992; Mardin et al., 2006; Shah et al., 2006).

A variety of risk factors may predispose an individual to either the development of Glaucoma or disease progression. The Ocular Hypertension Treatment Study (Gordon et al., 2002) suggested that several factors predisposed patients who had ocular hypertension without ophthalmoscopic or perimetric evidence of Glaucoma to develop Glaucoma. Patients who were older, had a larger cup-disc ratio at the start of the trial, greater elevation of IOP, or thinner corneas appeared to be more likely to develop Glaucoma. Pressure-independent factors that may predict the onset of Glaucoma or ocular hypertension may include genetic predisposition, altered optic-nerve microcirculation, systemic hypotension, race, or myopia (Gordon et al., 2002).

Quigley and collaborators observed histological evidence that there is a substantial loss of axons of the optic nerve before the first defects in the visual field appear (Quigley, 1985). Other studies have found clinical evidence of this same fact (Quigley et al., 1989; Sommer et al., 1991).

The functional studies performed today in clinical practice, fundamentally the conventional computerized perimetry (static, threshold, white stimulus on white background), do not appear to be optimal nor sufficiently sensitive to detect early functional damage in many individuals (Fig. 2). A high number of ocular hyper tense subjects and suspect of Glaucoma with normal standard visual fields present alterations of the visual function in other tests (Johnson et al., 1993; Sample et al., 1993).

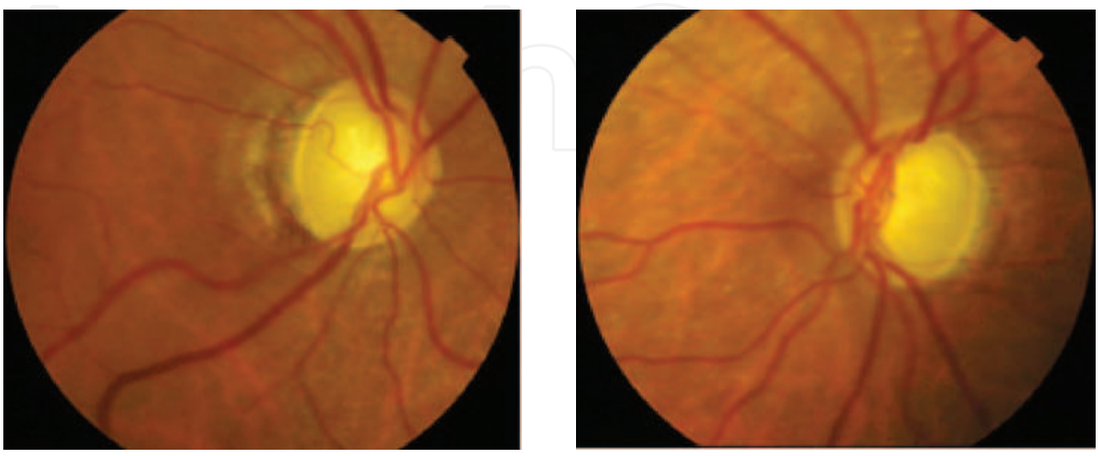

Fig. 1. Optic disc of a right and left eye from a patient with advanced glaucoma.

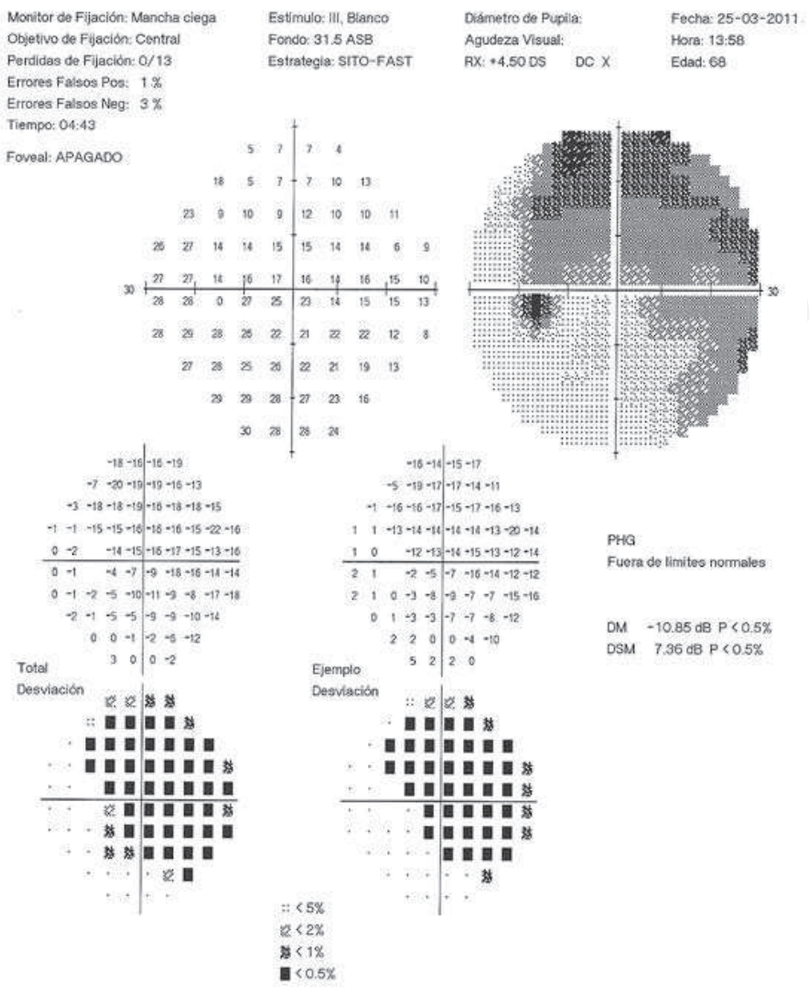

Fig. 2. Example for standard automated perimetry: Humphrey field analyzer test.

The single most effective method of diagnosing Glaucoma, therefore, is evaluating the optic nerve to determine if any injury has occurred. Direct examination of the optic nerve fibers at the optic nerve is essential in the diagnosis of Glaucoma, but is another non sensitive technique, in addition, normal eyes may have an optic nerve indistinguishable from those of incipient stages of Glaucoma. Other exploratory techniques are objective and reliable to detect Glaucoma before visual field loss, where search includes the technical photographic study of the layer of the retinal nerve fiber.

Today there is almost total unanimity in that the structural changes in the fiber layer of the retina and the neuro-retinal ring of the optic papilla precede the development of losses of visual field and it is admitted that the demonstration of specific alterations in the nerve fiber layer of the retina or in the papilla of the optic nerve allows the identification of a simple chronic Glaucoma in the most incipient phase of its clinical evolution independently of the ocular pressure and still in the absence of loss of visual field (Sharma et al., 2008; Tjon-Fo-Sang et al., 1996; Uchida et al., 1996; Weinreb et al., 1995).

Until now, the most universally accepted finding to establish a definitive diagnosis of Glaucoma was loss of visual field, but it is now considered that, even with more sophisticated

techniques, it requires a significant loss of optic nerve fibers to document the visual field loss (Sample et al., 1993). In Glaucoma optic neuropathy a progressive loss of retinal ganglion cells occurs and consequently a decrease in thickness of retinal nerve fibers layer. It is known that the decrease of these fibers begins up to five years before it functional damage established with perimetry can be detected. Functional and structural injury in Glaucoma is present and the measurements of changes in the optic nerve could be correlated with damage observed in the visual field. The availability of devices to allow the analysis of the thickness of the fibers layer is very important (Bowd et al., 2001; Shah et al., 2006).

As glaucomatous structural injury progresses, changes develop in the contour of the optic nerve. These features of glaucomatous optic neuropathy include diffuse or focal thinning of the neuroretinal rim, enlargement of the cup, notching, and/or excavation. Different methods have been used to document the status of the optic nerve and retinal nerve fiber layer, RNFL (Lin et al., 2007). The evaluation of the nerve fiber layer of the retina with photographic techniques has shown to have technical limitations and the possibility of high frequencies of false positives (Peli et al., 1986).

The direct exploration of the fibers by digital videoophthalmolgraphy of the peripapillar area described by Caprioli (Caprioli, 1990; Caprioli & Miller, 1988; 1989; Caprioli et al., 1989) was one of the first attempts to achieve an objective measure based on the digitalized images of the Rodenstock analyser. From the images of the retina surface and of a plane of reference in the retina surface itself the thickness of the RNFL is inferred. With this procedure Caprioli himself described, for the first time, the typical pattern of "camelÕs hump". Among the inconveniences the necessity of the reference plane is outstanding, which supposes the exigence that this be constant so that the measures of monitoring are valid since they originated a great variability of the measures obtained. This variability, nonetheless, is less than that of the measurements of the papilla structures performed in the comparative study of Miller & Caprioli (1991), which though it limits its clinical applications, demonstrates its utility.

Currently there are commercially available versions of optical imaging techniques (Figures 3 and 4): scanning laser polarimetry with variable corneal compensation (GDx VCC), confocal scanning laser ophthalmoscopy (HRT II, Heidelberg Retina Tomograph), and optical coherence tomography (Stratus OCT) to discriminate between healthy eyes and eyes with glaucomatous visual field loss. The sensitivities at high specificities were similar among the best parameters from each instrument (Medeiros et al., 2004).

Scanning laser polarimetry (SLP) is a technology used to assess the RNFL in order to detect early glaucomatous damage. This technology has several potential advantages. Because less biological variability is expected in the region of the RNFL than the optic-nerve head, clinicians have the ability to define a narrower range of normal RNFL measurements. SLP has another advantage, that of being independent of a reference plane. Therefore, the retardation value that is measured by SLP refers to the RNFL and is not dependent upon measurements of any other ocular region when considering change over a period of time (Medeiros et al., 2004; Weinreb et al., 1995).

Laser polarimetry is a technology that uses a polarized laser diode as light source (780 nm). It is a confocal ellipsometric laser measuring a total delay of light reflected from the retina and from these data determines the thickness of the RNFL (microns) point by point in the peripapillary region. Currently apparatus is being presented as a novelty compared to previous versions that can compensate corneal birefringence on an individual basis for each patient (Zhou, 2006).

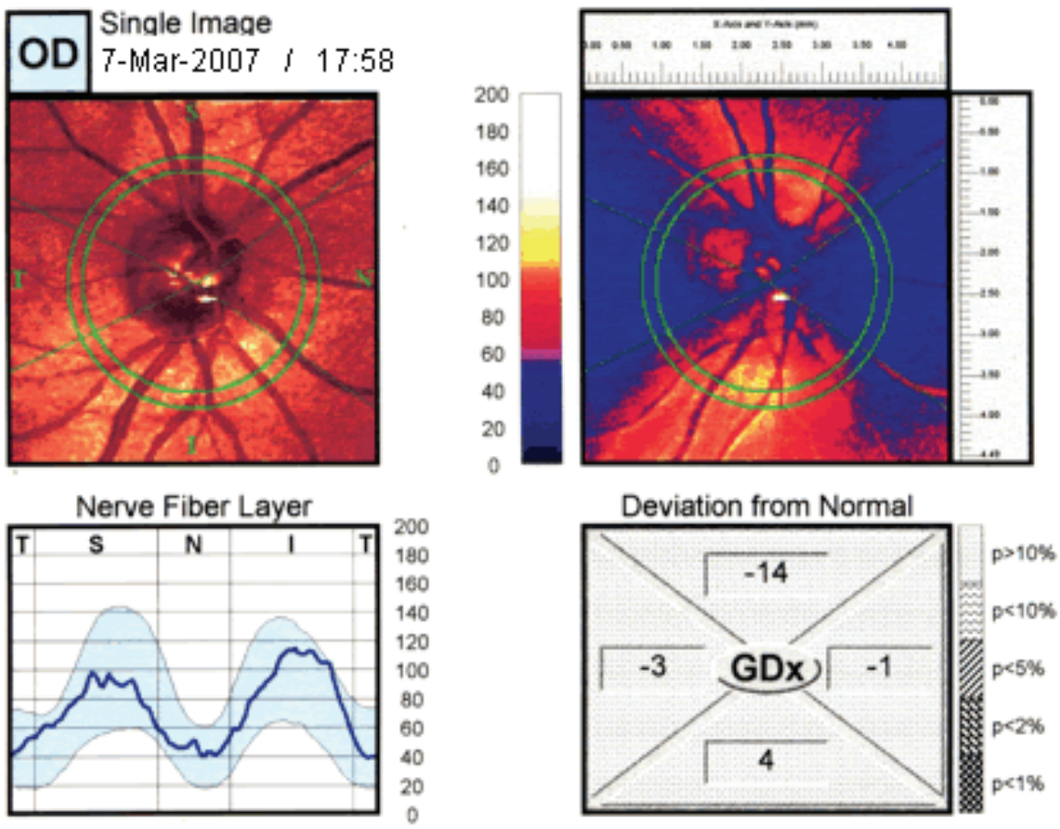

Fig. 3. Analysis with laser polarimetry for the measurement of the thickness of the layer of retinal nerve fibres using the NFA-II, GDX fibres analyser for a normal patient.

Scanning laser ophthalmoscopy. which is embodied in the Heidelberg Retinal Tomograph (Heidelberg Instruments, Inc., Heidelberg, Germany), is a highly reproducible technology that provides a means of obtaining objective measurements of optic-nerve topography. However, this technology was not fundamentally designed to generate RNFL assessments and there are limitations in relying on topography to detect glaucomatous progression (Bowd et al., 2002; Zangwill et al., 2001).

Another technology that has recently been utilized for Glaucoma detection is optical coherence tomocraphy, OCT (Fig. 5). OCT is a high resolution technology that generates direct measurements of the retina and RNFL thickness with a high degree of test-retest variability. However, few normative data for this technology exist at this time. OCT generates a single optical slice through the peripapillary RNFL, which may provide less information than a broad sampling of the entire RNFL profile provided by Scanning laser polarimetry (Burgansky-Eliash et al., 2005; Ferreras et al., 2008; Huang & Chen, 2005; Lu et al., 2008; Medeiros et al., 2005; 2004; Zangwill et al., 2001).

Glaucoma diagnosis is based on a range of normal measurements with the objective of finding eyes that are outside what is considered normal. There are two challenges for physicians when using structural testing. The first is diagnosis of the disease and the second is monitoring the known disease for progression.

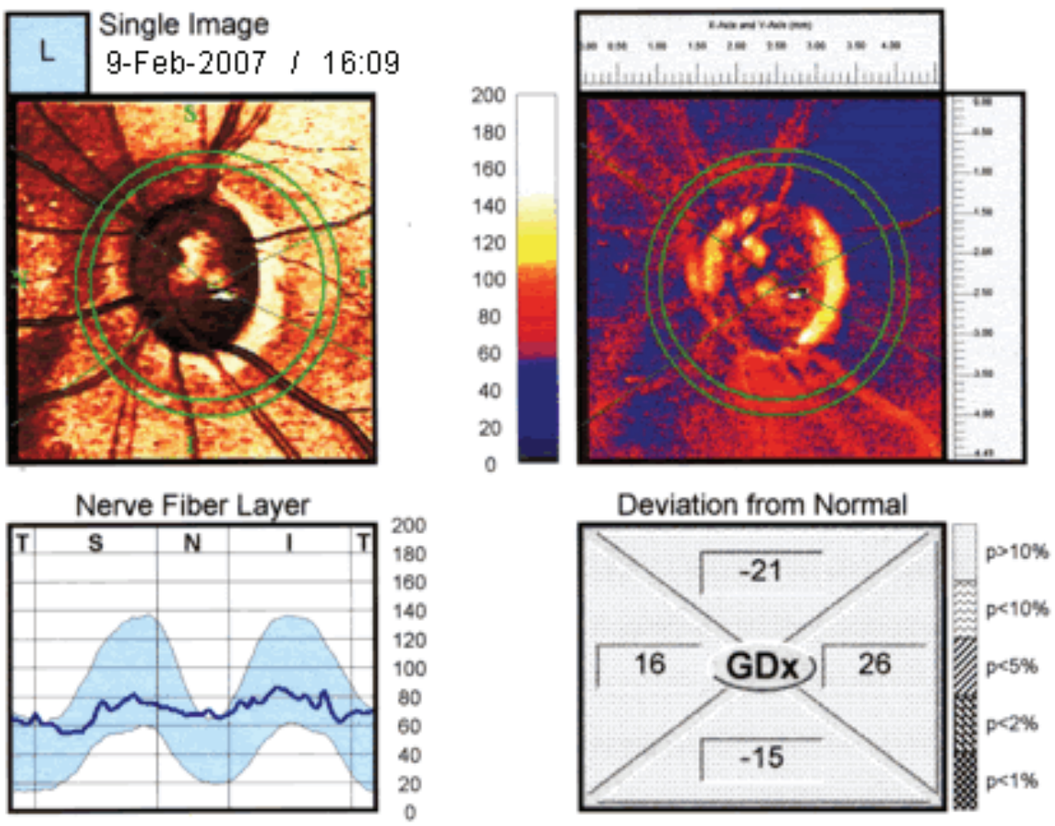

Fig. 4. Analysis with laser polarimetry for the measurement of the thickness of the layer of retinal nerve fibres using the NFA-II, GDX fibres analyser for a glaucomatous patient with stage 5 Glaucoma.

3. Diagnosis of Glaucoma by automatic systems

In ophthalmology applications of ANN have been used for the interpretation of the visual field for recognition and evaluation of the cell population of corneal endothelium (Ruggeri & Pajaro, 2002) and recognition of retinographs and angiofluorescent graphs in diabetic retinopathy (Gardner et al., 1996; Sivakumar et al., 2005).

Goldbaum et al. (1994) used the models of neuronal networks of multi-layer perceptron trained by retropropagation in the interpretation and classification of visual fields.

The methods of perimetric examination have contributed indices to analyze the visual field, but in no case was a clinical diagnosis included. The expert systems were the following step and were formed by programs specially designed to solve problems and to give diagnoses, taking into account the human experience accumulated. Based on the curve of accumulated defect, the indices and the influence of the false positives and negatives on the indices, they have been able to carry out classifications of the normal, doubtful or pathological visual fields in different degrees (Antón et al., 1995).

Other more complete programs integrated the analysis of the family and personal antecedents, the intraocular pressure, the papilla excavation indice and the state of the visual field, to similarly emit a clinical judgment.

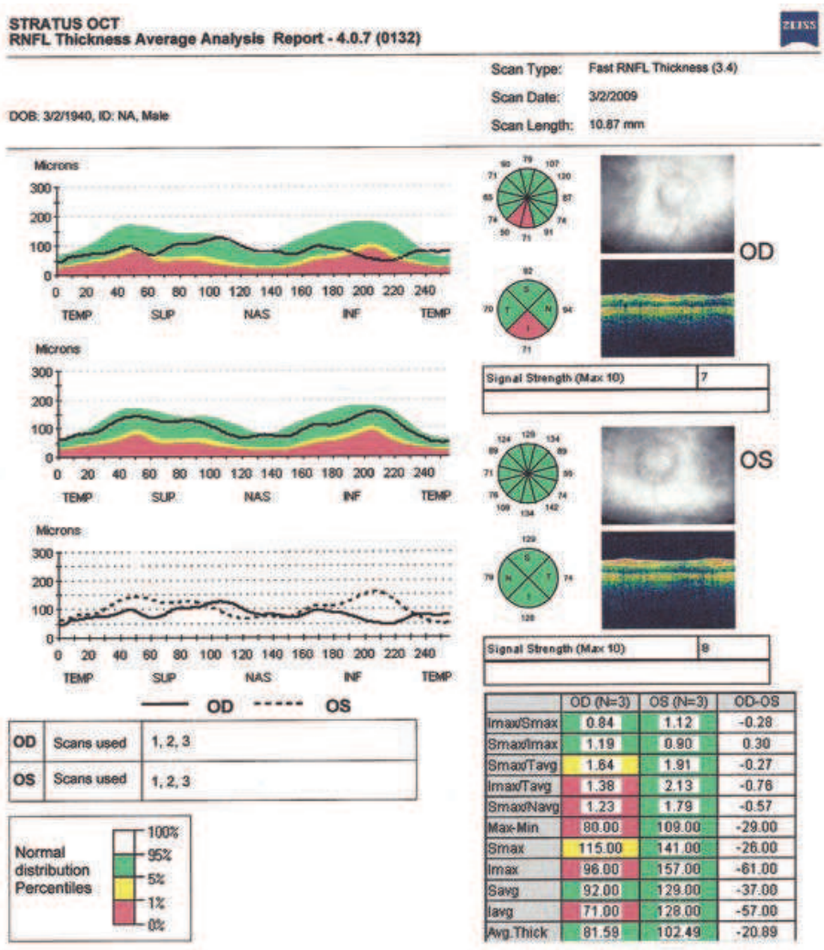

Fig. 5. Optical coherence tomography (OCT).

For the classification and diagnosis of the defects in the visual field a problem of discrimination into diagnostic categories has been proposed in accordance with the distribution and profundity of the lesions and, therefore, it is necessary to know the characteristics or patterns that allow the classification of each case. Moreover, the method chosen must be capable of treating qualitative and quantitative variables and perform with asymmetric variables of distribution or that are very distanced from a normal distribution. With these premises the list of usable procedures have been discriminant with logistic regression and the neuronal networks.

Antón et al. (1997) used the ANN for the interpretation of the incipient perimetric lesions produced in glaucoma and conclude that both the networks and the logistic regression are capable of differentiating between the incipient perimetric lesions produced by the glaucoma and those produced by other illnesses with important precision. They add that if these methods were applied to the PALOC, or another perimetric test, more sensitive to glaucomatous functional lesions than conventional perimetry, it would be a great aid for the identification and interpretation of the defects produced by this neuropathy.

Brigatti et al. (1996) also use the ANN to classify patients into normal or glaucomatous. They include automated data of the visual field, such as average defects, variances of corrected

losses and fluctuation in the short term, and structural data such as radius of excavation, volume of disc and thickness of the nerve fiber layer. On including the data for the visual field and the structural data the results are better than when the data are used separately. The sensitivity with the data together was 90% and the specificity 84%. Only with the structural data a sensitivity of 87% and specificity of 56% were achieved and the results were 84% and 86% respectively if only the functional data were trained.

Recently, the Ocular Hypertension Treatment Study has shown that approximately 50% of individuals who convert to glaucomatous optic neuropathy do not have detectable changes in standard automated perimetry. The results suggest that structural change precedes functional change. Therefore, a significant application of a different type of technology would provide a means of establishing a diagnosis of glaucoma prior to any detectable functional abnormalities in vision.

Artificial neural networks were reported to be able to differentiate between glaucoma and normal visual field status at least as well as trained readers (Bengtsson et al., 2005; Goldbaum et al., 1994; Lietman et al., 1999).

Artificial neural networks have been trained on different optic nerve head imaging analyzer parameters to classify eyes as glaucomatous or healthy in accordance with confocal scanning laser ophthalmoscopy (Brigatti et al., 1996; Uchida et al., 1996). Using this method, the neural network classifier is trained to detect a relationship between input (parameters of structural study) and a predefined gold-standard diagnosis by comparing its prediction with the labeled diagnosis and by learning from its mistakes.

Neural network techniques differ from basic statistical techniques such as linear discriminant function because they can adapt to the distribution of the data rather than assume a predefined distribution. The success of statistical or neural network classification methods is most often measured by reporting areas under the receiver operating characteristic curve or by reporting sensitivity at different specificities.

It was also reported that machine learning classifiers discriminate better between normal and glaucomatous fields than do global visual field indices (Goldbaum et al., 2002; Lietman et al., 1999). Global visual field indices are far from ideal as diagnostic tools, however, because they condense all threshold data into one number, resulting in loss of valuable spatial information, and visual field indices are not particularly sensitive to early localized glaucomatous visual field loss (Asman et al., 1992; Chauhan et al., 1989).

Disc topography data have also been added to visual field data to improve the diagnostic ability of ANNs (Brigatti et al., 1996).

Lietman et al. (1999) has determined a feed-forward neural network with a single hidden layer and was trained to recognize visual field defects previously collected in a longitudinal follow-up glaucoma study, and then tested on fields taken from the same study but not used in the training. The receiver operating characteristics of the network were then compared with the previously determined performance of other algorithms on the same data set.

ANNs have been suggested as tools for interpretation of automated visual field test results in patients with glaucoma (Goldbaum et al., 1994; Lietman et al., 1999). Other types of machine learning classifiers, such as support vector machines or committee machines, have also been reported to interpret visual fields adequately (Gordon et al., 2002).

Using the optic disc topography parameters of the Heidelberg Retina Tomograph neural network techniques can improve differentiation between glaucomatous and non-glaucomatous eyes. Trained neural networks, with global and regional Heidelberg Retina Tomograph parameters used as input, improve on previously proposed parameters for

discriminating between glaucomatous and nonglaucomatous eyes (AIGS, 2004; Bowd et al., 2002; 2001; 2004).
Neural networks and other machine classifiers seem to have a great potential to become a useful clinical tool in the diagnosis of glaucomatous visual field loss, and may be of value in the study of the performance of a range of types of data inputs with different machine classifiers.

4. Developing an artificial neural network

4.1 Neural networks

Rumelhart & McClelland (1986) presented the *backpropagation learning algorithm* in a year that can be considered the cornerstone of the ANNs recent history. ANN models have been extensively studied and applied in recent years in the hope of reaching human performance in different fields, including, for instance, automatic speech recognition, image processing, and biomedical applications (Arbib, 1995; Azuaje et al., 1999; Chan et al., 2002; Hernández Galilea et al., 2007; Lippmann & Kukolich, 1995; Lippmann & Shahian, 1997; Papalolukas et al., 2002; Peña Reyes & Sipper, 2000; Santos-García, 1990; Santos-García et al., 2004; Tu et al., 1998; Villar-Gómez & Santos-García, 1994; Widrow & Lehr, 1990). Actually, neurocomputing is blossoming almost daily in both theoretical and practical approaches. ANNs are generally more robust and outperform other computational tools in solving problems such as: classification, clustering, modeling, forecasting, optimization and association.
There are several models of neural nets according to their relevant features: topology, type of learning algorithm, degree of learning supervision, and so on. Classical ANN models are: Hopfield networks, Carpenter-Grossberg networks (Adaptative resonance theory), Kohonen networks (self-organizing feature maps), and backpropagation multilayer perceptron networks (Lippmann, 1987).
ANNs are empirical models in nature, however they obtain accurate and robust solutions for more or less precisely formulated problems and for complex phenomena that are only understood through experimental data.

4.2 Multilayer perceptron networks

A *neural network* is defined in mathematical terms as a graph with the following properties: (1) each node i, called *neuron* (Fig. 6), is associated with a state variable x_i storing its current output; (2) each junction between two neurons i and k, called *synapse* or *link*, is associated with a real weight ω_{ik}; (3) a real threshold θ_i, called *activation threshold*, is associated with each neuron i; (4) a *transfer function* $f_i[n_k, \omega_{ik}, \theta_i, (k \neq i)]$ is defined for each neuron, and determines the activation degree of the neuron as a function of its threshold, the weights of the input junctions and the outputs n_k of the neurons connected to its input synapses. In our case, the transfer function has the form $f(\sum_k \omega_{ik} n_k - \theta_i)$, where $f(x)$ is a sigmoidal function, defined by $f(x) = 1/(1 + e^{(\nu - x)})$, which corresponds to the continuous and derivable generalization of the step function (Hecht-Nielsen, 1990; Lippmann, 1987; Santos-García et al., 2008).
Multilayer perceptrons are networks with one or more layers of nodes between the layer of input units and the layer of output nodes; Fig. 7 shows a three-layer perceptron. These layers contain hidden units or nodes which obtain their input from the previous layer and output their results to the next layer, to both of which they are fully-connected. Nodes within each layer are not connected and have the same transfer function.
The strength of the multilayer perceptron originates from the use of non-linear sigmoidal functions in the nodes. If the nodes were linear elements, then monolayer networks with

appropriately selected weights could repeat the calculations carried out by a multilayer network (Widrow & Sterns, 1985). A multilayer perceptron with a non-linear step function and a hidden layer can solve problems in which the decision regions are open or closed convex regions. In the case of perceptrons with one hidden layer, problems with arbitrary decision regions can be solved, but more complex regions will need a greater number of nodes in the network (Hornik et al., 1995; Ilachinski, 2001).
Fundamental characteristics of a multilayer perceptron network are: (*i*) it is an adaptative method which permits the carrying out of non-linear statistics; (*ii*) fitting is made by a gradient method using the training data; (*iii*) a multilayer perceptron with three layers with step transference functions can solve any problem with arbitrary decision regions; (*iv*) noise in the patterns, the same as in the statistical fitting, does not impede their classification; (*v*) training of the connection weights must be very great; (*vi*) backpropagation algorithm usually finds the global minimum of the error function.

4.3 The backpropagation algorithm

The accuracy of the multilayer perceptron depends basically on the correct weights between nodes. The backpropagation training algorithm is an algorithm for adjusting those weights which uses a gradient descent method to minimize the mean quadratic error between the actual outputs of the perceptron and the desired outputs (Lippmann, 1987).
Let x_{ij}^k and y_{ij}^k be the input and output, respectively, for the i pattern of node j of layer k. Let ω_{ij}^k be the weight of the connection of neuron j of layer k with neuron i of the previous layer. By definition of the perceptron by layers, the following relationships are fulfilled

$$x_{ij}^k = \sum_l \omega_{lj}^k y_{il}^{k-1}; \;\; y_{ij}^k = f(x_{ij}^k)$$

The mean quadratic error function between the real output of the perceptron and the desired output, for a particular pattern i, is defined as $E_i = \frac{1}{2}\sum_{j,k}(y_{ij}^k - d_{ij}^k)^2$, where d_{ij}^k is the desired output for pattern i of node j of layer k. In order to minimize the error function we use the descending gradient function, considering the error function E_p and the weight sequence $\omega_{ij}^k(t)$, started randomly at time $t = 0$, and adapted to successive discrete time intervals. We then have $\omega_{ij}^k(t+1) = \omega_{ij}^k(t) - \eta\,\partial E_l / \partial \omega_{ij}^k(t)$, where η is the so-called *learning rate constant*.
We can conclude that $w_{ij}(t+1) = w_{ij}(t) + \eta\delta_j x_i'$, where x_i' is the output of neuron i, and δ_j is an error term for node j. For output neurons, it must be $\delta_j = y_j(1-y_j)(d_j - y_j)$. For a hidden node j, $\delta_j = x_j'(1-x_j')\sum_k \delta_k w_{jk}$, where k ranges over all neurons in the layers above neuron j. Internal node thresholds are adapted in a similar manner.

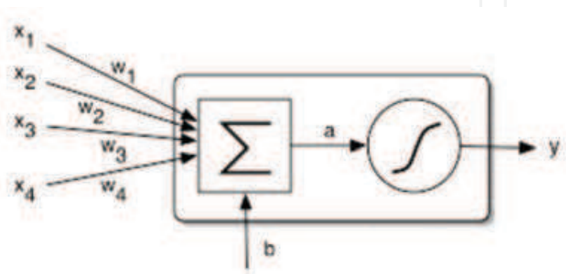

Fig. 6. Behaviour of an artificial neuron.

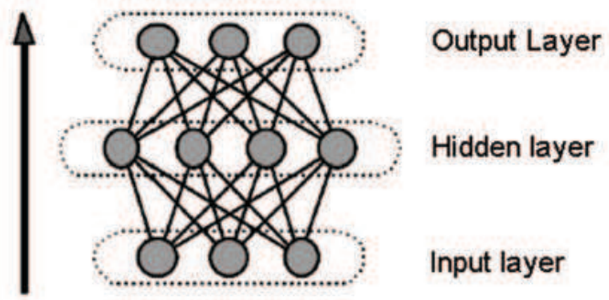

Fig. 7. A fully-connected, three-layer feed-forward perceptron neural network.

The high performance usually achieved with this backpropagation algorithm is rather surprising if we take into account the fact that the gradient method, of which the backpropagation training algorithm is a generalization, can find a local minimum of the error function instead of the desired global minimum. Some ideas for improving performance and reducing the appearance of local minimums are, for example, the addition of new nodes in the hidden layers, the lowering of the gain term used for the adaptation of weights and, above all, the initial training with a different set of random weights.

4.4 Matlab and Toolbox Neural Networks

Matlab (The MathWorks Inc, Natick, MA) is a high-level technical computing language and interactive environment for algorithm development, data visualization, data analysis, and numeric computation. It can be used in a wide range of applications, including signal and image processing, and computational biology. In an easily used environment Matlab integrates numerical analysis, the computation of matrices, the processing of signals and graphics, where the problems and solutions are expressed in a similar way to how they are expressed mathematically, avoiding the traditional programming. Matlab is an interactive system whose basic element of data is the matrix, which does not require to be dimensioned.
The Matlab language is a high-level matrix/array language with control flow statements, functions, data structures, input/output, and object-oriented programming features. It allows both *programming in the small* to rapidly create quick programs you do not intend to reuse. You can also do *programming in the large* to create complex application programs intended for reuse.
Neural Network Toolbox provides tools for designing, implementing, visualizing, and simulating neural networks. Neural Network Toolbox supports feedforward networks, radial basis networks, dynamic networks, self-organizing maps, and other proven network paradigms.
There are other work environments with neuronal networks. Some of them are Neural Works Professional II (Neural-Ware Inc., Pittsburgh, PA), SAS Enterprise Miner Software (SAS Institute Inc., Cary, NC), and Neural Connection (SPSS Inc., Chicago, IL).

5. ANN as a tool to identifier Glaucoma stages

For the diagnosis of Glaucoma, we propose a system of *Artificial Intelligence* that employs ANNs and integrates, jointly, the analysis of the nerve fibers of the retina from the study with scanning laser polarimetry (NFAII;GDx), perimetry and clinical data.
The present work shows an analysis of 106 eyes of 53 patients, in accordance with the stage of glaucomatous illness in which each eye was found. The groups defined include stage 0,

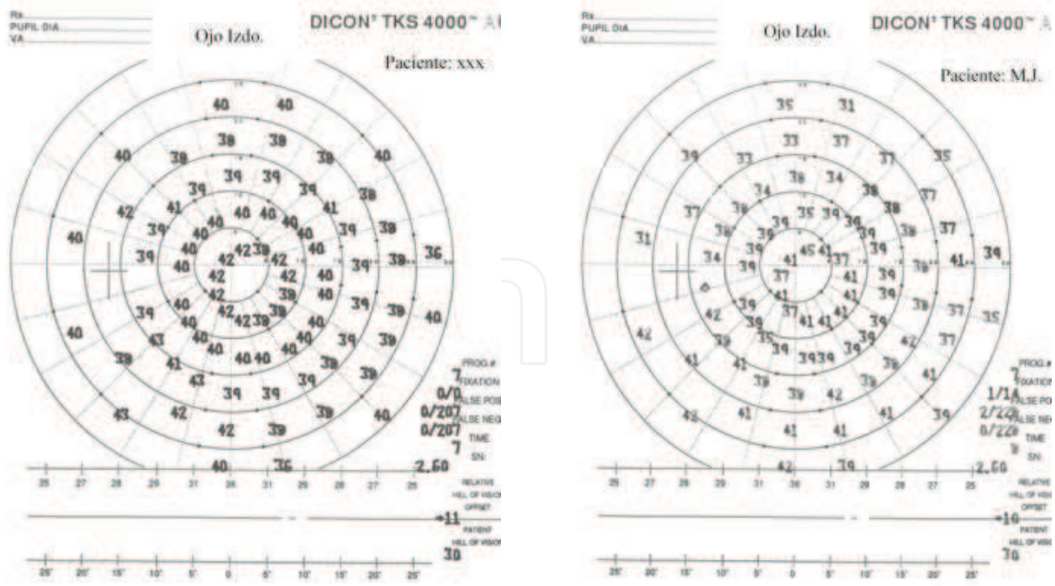

Fig. 8. Perimetry of a left eye of a normal patient (left image). Perimetry of a left eye of a patient (right image).

which corresponds to normal eyes; stage 1, for ocular hypertension; 2, for early Glaucoma; 3, for established Glaucoma; 4, for advanced Glaucoma and 5, for terminal Glaucoma. The developed ANN is a 16–30–1 multilayer perceptron provided with the Levenberg-Marquardt method (Franco Suárez-Bárcena et al., 2000; Lippmann, 1987; Widrow & Lehr, 1990).

5.1 Stages to classify

To classify the eyes in groups, besides studying IOP (Goldmann tonometry) and the ophthalmoscopic study of the optic disc by means of biometry using Volk aspheric lens (Quigley et al., 1994) Dicon TKS 4000 autoperimetry (Fig. 8) has been used for the analysis of the visual field and laser polarimetry for the measurement of the thickness of the layer of retinal nerve fibers using the NFA-II, GDX fiber analyser (Figures 3 and 4).

A classification into different groups was performed taking into account each eye of each patient separately. Thus, and taking into account the classification proposed by Caprioli (1992):

- Stage 0 (normal eye): Within this group were included patients whose IOP was lower than 21 mmHg and there was no effect on papilla nor the visual field nor of the parameters of the analyzer of the RNFL.
- Stage 1 (ocular hypertension): Formed by all the eyes that only presented an IOP equal to or greater than 21mmHg and both the exploration and the functional tests and the analysis of the RNFL were within normality.
- Stage 2 (early Glaucoma): They were eyes that presented an altered IOP and some of the following diagnostic data: effect on the papilla, incipient alteration of the visual field, decrease in the number of retinal nerve fibers.

- Stage 3 (established Glaucoma): Those eyes had IOP equal to or greater than 21 mmHg with involvement of the papilla, from moderate to significant alteration of the visual field as well as alteration of the RNFL analyzer parameters.
- Stage 4 (advanced Glaucoma): Those eyes that presented an IOP superior to 21 mmHg and an important effect, ophthalmoscopically demonstrable, on the papilla, an important alteration of the visual field and a significant alteration of the parameters of the analyser of RNFL.
- Stage 5 (terminal Glaucoma): If as well as the alterations in the IOP (equal to or greater than 21mmHg) there was papilla excavation with atrophy, the visual field with alterations proper to the terminal stage and alteration of the parameters of the analysis of the RNFL.

Table 1 shows a basic descriptive statistic by stage of the illness for the variables of study: Chamber, IOP, Papilla and Mean. These qualitative and quantitative variables are taken from the history and from the visual field of the individual. The intervals of confidence of the mean have been considered with a coefficient of confidence of 95%.

5.2 ANN variables

The input neurons receive the values of 16 input variables and the output neuron obtains the value of the output variable that corresponds with the stage of the Glaucoma for each eye. The definition of the 16 variables of input of the neuronal network consists of:

- **AGE**. Age of the patient.
- **CHAMBER**. Depth of the anterior chamber of the ocular globe.
- **IOP**. Intraocular pressure—expressed in millimetres of mercury.
- **OPTIC DISC**. Cup-to-disc ratio. If the result was less than 0.4, 0 was assigned; if between 0.4–0.5, 1 was assigned; if between 0.5–0.6, 2 was assigned and if between 0.7–0.9, 3 was assigned.

	CHAMBER *Depth of the chamber* (category)	**IOP** *Intraocular pressure* (mmHg)	**PAPILA** *Evaluation of the papilla (E/P)* (category)	**MEDIA** *Total mean of isopters of* 15°, 20°, 25°, 30°
STAGE 0 (normal eye)	$2,00 \pm 0,00$	$20,00 \pm 0,00$	$0,00 \pm 0,00$	$42,61 \pm 0,83$
STAGE 1 (ocular hypertension)	$2,00 \pm 0,36$	$22,29 \pm 0,70$	$0,00 \pm 0,00$	$41,70 \pm 1,85$
STAGE 2 (early Glaucoma)	$2,22 \pm 0,51$	$22,55 \pm 1,34$	$0,11 \pm 0,25$	$41,61 \pm 1,28$
STAGE 3 (established Glaucoma)	$2,13 \pm 0,25$	$23,96 \pm 0,89$	$0,93 \pm 0,10$	$40,39 \pm 1,32$
STAGE 4 (advanced Glaucoma)	$1,92 \pm 0,39$	$22,76 \pm 2,62$	$1,61 \pm 0,31$	$41,17 \pm 0,99$
STAGE 5 (terminal Glaucoma)	$1,93 \pm 0,21$	$25,21 \pm 2,61$	$1,54 \pm 0,31$	$39,07 \pm 2,80$
UNIVERSE	$2,02 \pm 0,12$	$23,63 \pm 0,89$	$0,94 \pm 0,16$	$40,49 \pm 1,00$

Table 1. Basic descriptive statistics by stage of illness for the variables of study: Chamber, IOP, Papilla and Mean. The intervals of confidence of the mean with coefficient of confidence of 95%.

- **FIXATION**. Fixation losses by the patient from all those performed during the autoperimetry testing of visual field examination.
- **NS, TS, NI, TI**. Average of the values of the visual field in the superior nasal, superior temporal, inferior nasal and inferior temporal quadrant, respectively.
- **MEAN**. Mean of all the values of the visual field.
- **NORMAL DEVIATION SUPERIOR, INFERIOR, TEMPORAL, NASAL**. Difference of the thickness of the nerve fibre layer employing the GDX program in the superior, inferior, temporal and nasal quadrant, respectively, for our patient compared with the normal patient of the same race and age.
- **NUMBER**. Experimental number extracted from all the values on acquiring an image employing NFA-II, GDX.
- **MEAN THICKNESS**. Mean of the thickness of all the pixels of the image; utilising the 65,536 points in an image considered valid.

The unaffected patients present a constant value in the variable of depth of the anterior chamber. The Mann-Whitney test establishes that there are no significant differences between the stage of illness groups for this variable. The graph of error for the variable chamber reveals that the different trustworthiness intervals of the affected patients overlap.

5.3 ANN results

The used ANN is a multilayer perceptron with backpropagation with a hidden layer provided with the Levenberg-Marquardt method. The input layer consists of 16 neurons, the hidden layer has 30 neurons and the output layer is a single neuron. The single neuron output layer with a logistic transfer function provided the network output: glaucomatous stage of the eye. The implementation of the ANN model has been carried out by means of the scientific computation platform R2010 *M*atlab, using the toolbox of *N*eural Networks (The MathWorks Inc, Natick, MA). Once the model had been defined, half the data were randomly employed to train the ANN. The learning was carried out with half of the data and with the training function of gradient descent w/momentum backpropagation and was checked by the diagnosis of an ophthalmologist, expert in glaucoma. The evolution of the process of learning is shown in Figure 9.

The model of neuronal network has been evaluated from the other half of the data. A 100% correct classification of each eye in the corresponding stage of glaucoma has been achieved. Therefore, the specificity and sensitivity are 100%.

With regard to the variable IOP, the unaffected patients take a constant value. There is a significant difference between the group of patients without illness and those affected regarding the variable IOP (p=0,001), according to the Mann-Whitney test. The graph of error for the variable IOP (Fig. 10) shows that the different intervals of confidence of the affected patients are overlapped among themselves.

The unaffected and ocular hypertense patients, which is to say, belonging to groups 0 and 1 do not present variation in the variable of relation excavation/papilla. There is a significant difference between the groups of subjects without illness and those affected with regard to the variable PAPILLA (p=0,004) according to the Mann-Whitney test.

Regarding the variable of mean, which represents the perimetric functional capacity and corresponds to the mean of all the values obtained from the visual field by autoperimetry there is a significant difference between the group of subjects without illness and the affected patients with respect to the mean variable (p=0,022), according to the Mann-Whitney test.

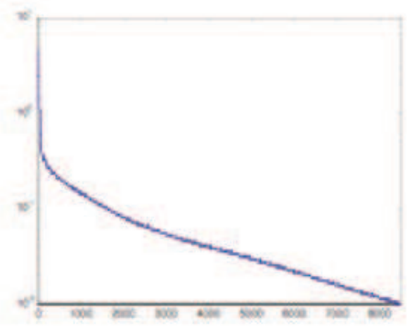

Fig. 9. Training evolution of our proposed ANN model.

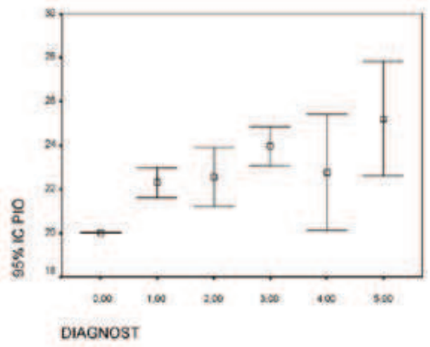

Fig. 10. Graph of error of the variable IOP referring to the Intraocular Pressure in mmHg for each of the groups (0,00 Stage 0 (normal eye): IOP was inferior to 21 mmHg; 1,00 Stage1 (ocular hypertension $\geq$ 21 mmHg; 2,00 Stage 2 (early Glaucoma); 3,00 Stage 3 (established Glaucoma); 4,00 Stage 4 (advanced Glaucoma); 5,00 Stage 5 (terminal Glaucoma)) of illness. The confidence intervals of the mean of coefficient of confidence of 95%.

6. Discussion

Glaucoma constitutes a pathology of multifactorial etiology, thus establishing an objective alteration in the different diagnostic tests represents the principal element for the performance of a certain diagnosis of glaucoma. This fact is especially transcendent in those situations in which the possible precocious diagnosis entails a therapeutic action which in a fundamental way affects the prognosis of the illness.

At present no diagnostic test can be considered alone and constitute in itself a diagnostic criterion. It is accepted that IOP is a risk factor, without being considered a specific and discriminatory element of glaucoma, in addition, when the term of normotensional or low pressure glaucoma has been established to define a variant in which the glaucomatous neuropathy takes place without the participation of an elevated pressure. Nonetheless, it continues to represent an objective clinical parameter and highly reproducible, clearly correlated with the development of the illness, being, moreover, one of the factors of risk which can be medically and surgically acted upon.

It is evident that in spite of the increase of specificity and sensitivity of the diagnostic tests which are applied to glaucoma, such as computerised perimetry or the analysis of the nerve fibers of the retina, clinical judgment persists as the primordial element, based on the

phenotypic characteristics of the patient, the clinical signs and monitoring, all performed by an expert evaluator in glaucoma.

With regard to the clinical significance, the most relevant datum of the exploration in glaucoma is the ophthalmoscopic evaluation of the papilla (Sommer et al., 1991). It is simple for an ophthalmologist to recognize a glaucomatous alteration of the papilla in the case of terminal (G4) or advanced (G5) glaucoma and even, in its case, to discriminate the papilla alteration for the group of established glaucoma (G3). Nevertheless, incipient alterations entail a greater difficulty in discrimination.

The cup-to-disc ratio has been considered a valid parameter to discriminate between normal and glaucomatous subjects as well as to quantify the progress of the disease. At present, however, another series of findings are included that complete the clinical evaluation, as are the disc haemorrhages in splinter, the presence of optic head notch, more frequent on the temporal side. This last has been considered as a relatively specific parameter of incipient glaucomatous damage (Fingeret et al., 2005).

The structural alterations produced in glaucoma can be determined through the study of clinical signs and the ophthalmic examination of the papilla. Nonetheless, the functional alterations are more precocious. These alterations are demonstrated in the study of the visual field which contributes the translation of the damage of ganglion cells of the retina in the context of glaucomatous illness.

We therefore consider that even when the mean functional capacity is not the only parameter to be evaluated it results, in our study to be a relatively non-specific datum as it is unable to differentiate between the different groups in accordance with the stages of the glaucomatous illness. Nevertheless, and even when the criteria of selection were sufficient to not include defects of refraction, opacities of lens or artefacts, due to other pathologies, this fact has not influenced, in a fundamental manner, the results of the autoperimetry.

The variability of the perimetry as an exploratory method, as well as the lack of reproducibility, is one of its principal inconveniences. Perhaps the most important is that it is a subjective test that, moreover, depends on the training and collaboration of the patient. This fact is even more important in the present forms of perimetry whose test is of greater complexity than that of the conventional one (Racette et al., 2008; Sakata et al., 2007).

Autoperimetry is a very simplified method regarding training of the patient and monitoring of the test, allowing its management by unqualified personnel. Moreover, it is performed in a short period of time. The interpretation of the field is relatively simple and comparable with conventional perimetries, using a more simple series of algorithms, they cannot be compared with the more diffused standards of the computerized perimeters, nonetheless permit a rapid interpretation.

The evaluation of the campimetric defects, however, are not exclusively based on the quantitative results, but also on the qualitative characteristics, such as the location, shape and extension of the scotomas. The diagnostic efficiency is greater when the indexes that incorporate these characteristics are considered (Sommer et al., 1991).

The incipient lesions do not present a high specificity, thus the interpretation of a visual field lacks objectivity and is based both on the clinical experience from which the results are analysed and from the evaluation of the contralateral eye and the performance of the test on more occasions.

For all these reasons the use of a system of Artificial Intelligence has been proposed so that analysing the parameters obtained in the perimetry such as the indexes and spatial

considerations it will be possible to produce a diagnosis (Burgansky-Eliash et al., 2005; Henson et al., 1997; Huang & Chen, 2005).

Diverse authors have developed neuronal networks and confirmed their utility in the differentiation and spatial classification of the perimetric defects, after training the neuronal network and an index of specificity and sensitivity of over 80% has been established in the different studies (Antón et al., 1997; Henson et al., 1997).

In our study, and commencing from the efficacy of the systems of neuronal networks applied to the recognition of the visual fields in glaucomatous pathology we have performed the design of a neuronal network with the objective of, employing the great quantity of indexes, parameters, variables and algorithms derived from the autoperimetry and the analysis of the CNFR by laser polarimetry, being able to carry out an assignation of patients in the diverse subgroups of evolution of the primary glaucoma of open angle.

At present the clinical exploration does not contribute sufficient data to produce a diagnosis or establish the adequate stage of evolution. Equally it is not possible to differentiate among the group of ocular hypertension Those who should be treated, since later they develop a glaucoma. This possibility of discrimination at present settles in an essential manner, in functional tests like perimetry or in the objective quantification of the structural damage of the optic nerve. Similarly, none of these tests can be considered in an isolated fashion, as we have mentioned previously. Even when both possess a high index of correlation it is not possible to forego the data from clinical exploration to perform a certain diagnosis. In addition, in the interpretation of the clinical and quantitative data it is necessary in all cases that an expert participates which in many cases is found in the context of the exploration (Bowd et al., 2002; 2005; Goldbaum et al., 2005; Shah et al., 2006; Zhu et al., 2010).

In the neuronal network designed for our study a total of 16 variables of work were used which formed the inputs for the neuronal network, establishing the diagnosis as the only variable of output of the model. The layer of neurons of input was composed by indices of polarimetry together with parameters from the autoperimetry and those derived from the clinical exploration. The occult/hidden layer was composed by thirty nodes or neurons and a single output to constitute a neuronal network of multilayer perceptron with retropropagation.

For the function of training the data of 50% of the patients of our data base were used including normal and glaucomatous patients in diverse stages at random, achieving with a total of 8000 cycles an adequate model to achieve the threshold of mean error of the neuronal network. The performance of classification of the designed network was validated with the remainder of the data of the other 50% of the patients of the database.

We have been able to prove that the assignation to each of the subgroups of evolution of glaucoma was 100% achieving a specificity and sensitivity of 100%. Mutlukan & Keating (1994) achieves similar percentages with a neuronal network of retropropagation designed for the identification of visual fields with three layers with a hidden layer of 40 nodes.

The updating and improvement of technological tools of systems like Bayesian machine learning (Boden et al., 2007; Bowd et al., 2008) or the neuronal networks where the interpretation of structural methods such as optical coherence tomography or GDx polarimetry and functional ones such as standard automated perimetry can be combined will increase the yield in the detection of glaucoma and its progression.

7. References

AIGS (2004). Glaucoma diagnosis structure and function reports and consensus statements, *1st Global AIGS Consensus Meeting on Structure and Function in the Management of Glaucoma*, Kugler Publications, Amsterdam.

Antón, A., Jordano, J. & Maquet, J. (1995). Sistema experto de diagnóstico de glaucoma: "glaucom easy", *Archivos de la Sociedad Española de Oftalmología* **69**: 23–28.

Antón, A., Zangwill, L., Emdadi, A. & Weinreb, R. N. (1997). Nerve fiber layer measurements with scanning laser polarimetry in ocular hypertension, *Arch Ophthalmol* **115**(3): 331–4.

Arbib, M. (1995). *Handbook of brain theory and neural netwoks*, MIT Press, Cambridge, MA.

Asman, P., Heijl, A., Olsson, J. & Rootzen, H. (1992). Spatial analyses of glaucomatous visual fields; a comparison with traditional visual field indices, *Acta Ophthalmol (Copenh)* **70**(5): 679–86.

Azuaje, F., Dubitzky, W., Lopes, P., Black, N., Adamson, K., Wu, X. & White, J. A. (1999). Predicting coronary disease risk based on short-term rr interval measurements: a neural network approach, *Artif Intell Med* **15**(3): 275–97.

Bengtsson, B., Bizios, D. & Heijl, A. (2005). Effects of input data on the performance of a neural network in distinguishing normal and glaucomatous visual fields, *Invest Ophthalmol Vis Sci* **46**(10): 3730–6.

Boden, C., Chan, K., Sample, P. A., Hao, J., Lee, T. W., Zangwill, L. M., Weinreb, R. N. & Goldbaum, M. H. (2007). Assessing visual field clustering schemes using machine learning classifiers in standard perimetry, *Invest Ophthalmol Vis Sci* **48**(12): 5582–90.

Bowd, C., Chan, K., Zangwill, L. M., Goldbaum, M. H., Lee, T. W., Sejnowski, T. J. & Weinreb, R. N. (2002). Comparing neural networks and linear discriminant functions for glaucoma detection using confocal scanning laser ophthalmoscopy of the optic disc, *Invest Ophthalmol Vis Sci* **43**(11): 3444–54.

Bowd, C., Hao, J., Tavares, I. M., Medeiros, F. A., Zangwill, L. M., Lee, T. W., Sample, P. A., Weinreb, R. N. & Goldbaum, M. H. (2008). Bayesian machine learning classifiers for combining structural and functional measurements to classify healthy and glaucomatous eyes, *Invest Ophthalmol Vis Sci* **49**(3): 945–53.

Bowd, C., Medeiros, F. A., Zhang, Z., Zangwill, L. M., Hao, J., Lee, T. W., Sejnowski, T. J., Weinreb, R. N. & Goldbaum, M. H. (2005). Relevance vector machine and support vector machine classifier analysis of scanning laser polarimetry retinal nerve fiber layer measurements, *Invest Ophthalmol Vis Sci* **46**(4): 1322–9.

Bowd, C., Zangwill, L. M., Berry, C. C., Blumenthal, E. Z., Vasile, C., Sanchez-Galeana, C., Bosworth, C. F., Sample, P. A. & Weinreb, R. N. (2001). Detecting early glaucoma by assessment of retinal nerve fiber layer thickness and visual function, *Invest Ophthalmol Vis Sci* **42**(9): 1993–2003.

Bowd, C., Zangwill, L. M., Medeiros, F. A., Hao, J., Chan, K., Lee, T. W., Sejnowski, T. J., Goldbaum, M. H., Sample, P. A., Crowston, J. G. & Weinreb, R. N. (2004). Confocal scanning laser ophthalmoscopy classifiers and stereophotograph evaluation for prediction of visual field abnormalities in glaucoma-suspect eyes, *Invest Ophthalmol Vis Sci* **45**(7): 2255–62.

Brigatti, L., Hoffman, D. & Caprioli, J. (1996). Neural networks to identify glaucoma with structural and functional measurements, *Am J Ophthalmol* **121**(5): 511–21.

Burgansky-Eliash, Z., Wollstein, G., Chu, T., Ramsey, J. D., Glymour, C., Noecker, R. J., Ishikawa, H. & Schuman, J. S. (2005). Optical coherence tomography machine

learning classifiers for glaucoma detection: a preliminary study, *Invest Ophthalmol Vis Sci* **46**(11): 4147–52.

Caprioli, J. (1990). The contour of the juxtapapillary nerve fiber layer in glaucoma, *Ophthalmology* **97**(3): 358–65; discussion 365–6.

Caprioli, J. (1992). Discrimination between normal and glaucomatous eyes, *Invest Ophthalmol Vis Sci* **33**(1): 153–9.

Caprioli, J. & Miller, J. M. (1988). Videographic measurements of optic nerve topography in glaucoma, *Invest Ophthalmol Vis Sci* **29**(8): 1294–8.

Caprioli, J. & Miller, J. M. (1989). Measurement of relative nerve fiber layer surface height in glaucoma, *Ophthalmology* **96**(5): 633–39; discussion 639–41.

Caprioli, J., Ortiz-Colberg, R., Miller, J. M. & Tressler, C. (1989). Measurements of peripapillary nerve fiber layer contour in glaucoma, *Am J Ophthalmol* **108**(4): 404–13.

Chan, K., Lee, T. W., Sample, P. A., Goldbaum, M. H., Weinreb, R. N. & Sejnowski, T. J. (2002). Comparison of machine learning and traditional classifiers in glaucoma diagnosis, *IEEE Trans Biomed Eng* **49**(9): 963–74.

Chauhan, B. C., Drance, S. M. & Lai, C. (1989). A cluster analysis for threshold perimetry, *Graefes Arch Clin Exp Ophthalmol* **227**(3): 216–20.

European Glaucoma Society, E. (2008). *Terminology and Guidelines for Glaucoma*, Ed. Dogma, Savona, Italy.

Ferreras, A., Pablo, L. E., Pajarin, A. B., Larrosa, J. M., Polo, V. & Honrubia, F. M. (2008). Logistic regression analysis for early glaucoma diagnosis using optical coherence tomography, *Arch Ophthalmol* **126**(4): 465–70.

Fingeret, M., Medeiros, F. A., Susanna, R., J. & Weinreb, R. N. (2005). Five rules to evaluate the optic disc and retinal nerve fiber layer for glaucoma, *Optometry* **76**(11): 661–8.

Franco Suárez-Bárcena, I., Santos-García, G., E., H. G. & A., F. S. (2000). Aplicación de redes neuronales a la clasificación clínica en estadíos de glaucoma, *76 Congreso de la Sociedad Española de Oftalmología*, Madrid.

Gardner, G. G., Keating, D., Williamson, T. H. & Elliott, A. T. (1996). Automatic detection of diabetic retinopathy using an artificial neural network: a screening tool, *Br J Ophthalmol* **80**(11): 940–4.

Goldbaum, M. H., Sample, P. A., Chan, K., Williams, J., Lee, T. W., Blumenthal, E., Girkin, C. A., Zangwill, L. M., Bowd, C., Sejnowski, T. & Weinreb, R. N. (2002). Comparing machine learning classifiers for diagnosing glaucoma from standard automated perimetry, *Invest Ophthalmol Vis Sci* **43**(1): 162–9.

Goldbaum, M. H., Sample, P. A., White, H., Colt, B., Raphaelian, P., Fechtner, R. D. & Weinreb, R. N. (1994). Interpretation of automated perimetry for glaucoma by neural network, *Invest Ophthalmol Vis Sci* **35**(9): 3362–73.

Goldbaum, M. H., Sample, P. A., Zhang, Z., Chan, K., Hao, J., Lee, T. W., Boden, C., Bowd, C., Bourne, R., Zangwill, L., Sejnowski, T., Spinak, D. & Weinreb, R. N. (2005). Using unsupervised learning with independent component analysis to identify patterns of glaucomatous visual field defects, *Invest Ophthalmol Vis Sci* **46**(10): 3676–83.

Gordon, M. O., Beiser, J. A., Brandt, J. D., Heuer, D. K., Higginbotham, E. J., Johnson, C. A., Keltner, J. L., Miller, J. P., Parrish, R. K., n., Wilson, M. R. & Kass, M. A. (2002). The ocular hypertension treatment study: baseline factors that predict the onset of primary open-angle glaucoma, *Arch Ophthalmol* **120**(6): 714–20; discussion 829–30.

Hecht-Nielsen, R. (1990). *Neurocomputing*, Addison-Wesley, Reading, MA.

Henson, D. B., Spenceley, S. E. & Bull, D. R. (1997). Artificial neural network analysis of noisy visual field data in glaucoma, *Artif Intell Med* **10**(2): 99–113.

Hernández Galilea, E., Santos-García, G. & Suárez-Bárcena, I. (2007). Identification of glaucoma stages with artificial neural networks using retinal nerve fibre layer analysis and visual field parameters, *in* E. Corchado, J. Corchado & A. Abraham (eds), *Innovations in Hybrid Intelligent Systems*, Vol. 44 of *Advances in Intelligent and Soft Computing*, Springer Berlin / Heidelberg, pp. 418–424.

Hornik, K., Stinchcombe, M., White, H. & Auer, P. (1995). Degree of approximation results for feedforward networks approximating unknown mappings and their derivatives, *Neural Computation* **6**(6): 1262–1275.

Huang, M. L. & Chen, H. Y. (2005). Development and comparison of automated classifiers for glaucoma diagnosis using stratus optical coherence tomography, *Invest Ophthalmol Vis Sci* **46**(11): 4121–9.

Ilachinski, A. (2001). *Cellular automata*, World Scientific Publishing Company.

Johnson, C. A., Adams, A. J., Casson, E. J. & Brandt, J. D. (1993). Blue-on-yellow perimetry can predict the development of glaucomatous visual field loss, *Arch Ophthalmol* **111**(5): 645–50.

Lietman, T., Eng, J., Katz, J. & Quigley, H. A. (1999). Neural networks for visual field analysis: how do they compare with other algorithms?, *J Glaucoma* **8**(1): 77–80.

Lin, S. C., Singh, K., Jampel, H. D., Hodapp, E. A., Smith, S. D., Francis, B. A., Dueker, D. K., Fechtner, R. D., Samples, J. S., Schuman, J. S. & Minckler, D. S. (2007). Optic nerve head and retinal nerve fiber layer analysis: a report by the american academy of ophthalmology, *Ophthalmology* **114**(10): 1937–49.

Lippmann, R. (1987). An introduction to computing with neural nets, *IEEE ASSP Magazine* **4**: 4–22.

Lippmann, R. & Kukolich, L. (1995). Using neural networks to predict the risk of cardiac bypass operations, *in* S. Rogers & D. Ruck (eds), *Applications and science of artificial neural networks*, SPIE, pp. 650–660.

Lippmann, R. P. & Shahian, D. M. (1997). Coronary artery bypass risk prediction using neural networks, *Ann Thorac Surg* **63**(6): 1635–43.

Lu, A. T., Wang, M., Varma, R., Schuman, J. S., Greenfield, D. S., Smith, S. D. & Huang, D. (2008). Combining nerve fiber layer parameters to optimize glaucoma diagnosis with optical coherence tomography, *Ophthalmology* **115**(8): 1352–7, 1357 e1–2.

Mardin, C. Y., Peters, A., Horn, F., Junemann, A. G. & Lausen, B. (2006). Improving glaucoma diagnosis by the combination of perimetry and hrt measurements, *J Glaucoma* **15**(4): 299–305.

Medeiros, F. A., Zangwill, L. M., Bowd, C., Vessani, R. M., Susanna, R., J. & Weinreb, R. N. (2005). Evaluation of retinal nerve fiber layer, optic nerve head, and macular thickness measurements for glaucoma detection using optical coherence tomography, *Am J Ophthalmol* **139**(1): 44–55.

Medeiros, F. A., Zangwill, L. M., Bowd, C. & Weinreb, R. N. (2004). Comparison of the gdx vcc scanning laser polarimeter, hrt ii confocal scanning laser ophthalmoscope, and stratus oct optical coherence tomograph for the detection of glaucoma, *Arch Ophthalmol* **122**(6): 827–37.

Miller, E. & Caprioli, J. (1991). Regional and long-term variability of fundus measurements made with computer-image analysis, *Am J Ophthalmol* **112**(2): 171–6.

Mutlukan, E. & Keating, D. (1994). Visual field interpretation with a personal computer based neural network, *Eye (Lond)* **8 (Pt 3)**: 321–3.

Papalolukas, C., Fotiadis, D. I., Likas, A. & Michalis, L. K. (2002). An ischemia detection method based on artificial neural networks, *Artif Intell Med* **24**: 167–178.

Peña Reyes, C. A. & Sipper, M. (2000). Evolutionary computation in medicine: an overview, *Artif Intell Med* **19**: 1–23.

Peli, E., Hedges, T. R. & Schwartz, B. (1986). Computerized enhancement of retinal nerve fiber layer, *Acta Ophthalmol (Copenh)* **64**(2): 113–22.

Quigley, H. A. (1985). Better methods in glaucoma diagnosis, *Arch Ophthalmol* **103**(2): 186–9.

Quigley, H. A., Dunkelberger, G. R. & Green, W. R. (1989). Retinal ganglion cell atrophy correlated with automated perimetry in human eyes with glaucoma, *Am J Ophthalmol* **107**(5): 453–64.

Quigley, H. A., Enger, C., Katz, J., Sommer, A., Scott, R. & Gilbert, D. (1994). Risk factors for the development of glaucomatous visual field loss in ocular hypertension, *Arch Ophthalmol* **112**(5): 644–9.

Racette, L., Medeiros, F. A., Zangwill, L. M., Ng, D., Weinreb, R. N. & Sample, P. A. (2008). Diagnostic accuracy of the matrix 24-2 and original n-30 frequency-doubling technology tests compared with standard automated perimetry, *Invest Ophthalmol Vis Sci* **49**(3): 954–60.

Ruggeri, A. & Pajaro, S. (2002). Automatic recognition of cell layers in corneal confocal microscopy images, *Comput Methods Programs Biomed* **68**(1): 25–35.

Rumelhart, D. & McClelland, J. (1986). *Parallel distributed processing*, MIT Press, Cambridge, MA.

Sakata, L. M., Deleon-Ortega, J., Arthur, S. N., Monheit, B. E. & Girkin, C. A. (2007). Detecting visual function abnormalities using the swedish interactive threshold algorithm and matrix perimetry in eyes with glaucomatous appearance of the optic disc, *Arch Ophthalmol* **125**(3): 340–5.

Sample, P. A., Taylor, J. D., Martinez, G. A., Lusky, M. & Weinreb, R. N. (1993). Short-wavelength color visual fields in glaucoma suspects at risk, *Am J Ophthalmol* **115**(2): 225–33.

Santos-García, G. (ed.) (1990). *The Hopfield and Hamming networks applied to the automatic speech recognition of the five Spanish vowels*, Artificial Neural Nets and Genetic Algorithms, Springer-Verlag, Wien.

Santos-García, G., Palomino, M. & Verdejo, A. (2008). Rewriting logic using strategies for neural networks: an implementation in maude, *in* J. M. Corchado, S. Rodríguez, J. Llinas & J. M. Molina (eds), *International Symposium on Distributed Computing and Artificial Intelligence (DCAI 2008)*, Vol. 50 of *Advances in Soft Computing*, Springer, Salamanca, pp. 424–433.

Santos-García, G., Varela, G., Novoa, N. & Jiménez, M. F. (2004). Prediction of postoperative morbidity after lung resection using an artificial neural network ensemble, *Artificial Intelligence in Medicine* **30**(1): 61–69.

Shah, N. N., Bowd, C., Medeiros, F. A., Weinreb, R. N., Sample, P. A., Hoffmann, E. M. & Zangwill, L. M. (2006). Combining structural and functional testing for detection of glaucoma, *Ophthalmology* **113**(9): 1593–602.

Sharma, P., Sample, P. A., Zangwill, L. M. & Schuman, J. S. (2008). Diagnostic tools for glaucoma detection and management, *Surv Ophthalmol* **53 Suppl1**: S17–32.

Shields, M. B. (1992). *Textbook of glaucoma*, 3rd ed edn, : Williams & Wilkins, Baltimore [etc.].

Sivakumar, R., Ravindran, G., Muthayya, M., Lakshminarayanan, S. & Velmurughendran, C. U. (2005). Diabetic retinopathy analysis, *J Biomed Biotechnol* **2005**(1): 20–27.

Sommer, A., Katz, J., Quigley, H. A., Miller, N. R., Robin, A. L., Richter, R. C. & Witt, K. A. (1991). Clinically detectable nerve fiber atrophy precedes the onset of glaucomatous field loss, *Arch Ophthalmol* **109**(1): 77–83.

Song, X., Song, K. & Chen, Y. (2005). A computer-based diagnosis system for early glaucoma screening, *Conf Proc IEEE Eng Med Biol Soc* **6**: 6608–11.

Tjon-Fo-Sang, M. J., de Vries, J. & Lemij, H. G. (1996). Measurement by nerve fiber analyzer of retinal nerve fiber layer thickness in normal subjects and patients with ocular hypertension, *Am J Ophthalmol* **122**(2): 220–7.

Tu, J. V., Weinstein, M. C., McNeil, B. J. & Naylor, C. D. (1998). Predicting mortality after coronary artery bypass surgery: what do artificial neural networks learn? the steering committee of the cardiac care network of ontario, *Med Decis Making* **18**(2): 229–35.

Uchida, H., Brigatti, L. & Caprioli, J. (1996). Detection of structural damage from glaucoma with confocal laser image analysis, *Invest Ophthalmol Vis Sci* **37**(12): 2393–401.

Villar-Gómez, R. & Santos-García, G. (1994). Multilayer perceptron applied to the automatic speech recognition of the spanish vowels, *Sci Bull, Ser A: Appl Math Phys* **56**.

Weinreb, R. N., Shakiba, S. & Zangwill, L. (1995). Scanning laser polarimetry to measure the nerve fiber layer of normal and glaucomatous eyes, *Am J Ophthalmol* **119**(5): 627–36.

Widrow, B. & Lehr, M. (1990). 30 years of adaptative neural networks: Perceptron, madaline, and backpropagation, *Proceedings of the IEEE*, Vol. 78, pp. 1415–1442.

Widrow, B. & Sterns, S. (1985). *Adaptive signal processing*, Prentice Hall.

Zangwill, L. M., Bowd, C., Berry, C. C., Williams, J., Blumenthal, E. Z., Sanchez-Galeana, C. A., Vasile, C. & Weinreb, R. N. (2001). Discriminating between normal and glaucomatous eyes using the heidelberg retina tomograph, gdx nerve fiber analyzer, and optical coherence tomograph, *Arch Ophthalmol* **119**(7): 985–93.

Zhou, Q. (2006). Retinal scanning laser polarimetry and methods to compensate for corneal birefringence, *Bull Soc Belge Ophtalmol* **302**: 89–106.

Zhu, H., Crabb, D. P., Schlottmann, P. G., Lemij, H. G., Reus, N. J., Healey, P. R., Mitchell, P., Ho, T. & Garway-Heath, D. F. (2010). Predicting visual function from the measurements of retinal nerve fiber layer structure, *Invest Ophthalmol Vis Sci* **51**(11): 5657–66.

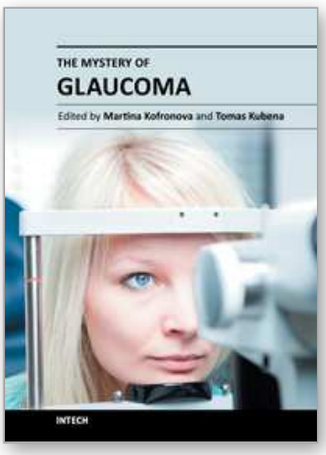

The Mystery of Glaucoma
Edited by Dr. Tomas Kubena

ISBN 978-953-307-567-9
Hard cover, 352 pages
Publisher InTech
Published online 06, September, 2011
Published in print edition September, 2011

Since long ago scientists have been trying hard to show up the core of glaucoma. To its understanding we needed to penetrate gradually to its molecular level. The newest pieces of knowledge about the molecular biology of glaucoma are presented in the first section. The second section deals with the clinical problems of glaucoma. Ophthalmologists and other medical staff may find here more important understandings for doing their work. What would our investigation be for, if not owing to the people's benefit? The third section is full of new perspectives on glaucoma. After all, everybody believes and relies – more or less – on bits of hopes of a better future. Just let us engage in the mystery of glaucoma, to learn how to cure it even to prevent suffering from it. Each information in this book is an item of great importance as a precious stone behind which genuine, through and honest piece of work should be observed.

InTech Europe
University Campus STeP Ri
Slavka Krautzeka 83/A
51000 Rijeka, Croatia
Phone: +385 (51) 770 447
Fax: +385 (51) 686 166
www.intechopen.com

InTech China
Unit 405, Office Block, Hotel Equatorial Shanghai
No.65, Yan An Road (West), Shanghai, 200040, China
中国上海市延安西路65号上海国际贵都大饭店办公楼405单元
Phone: +86-21-62489820
Fax: +86-21-62489821

IntechOpen